

PAPER • OPEN ACCESS

XPS Depth Profiling of Air-Oxidized Nanofilms of NbN on GaN Buffer-Layers

To cite this article: A.V. Lubenchenko *et al* 2017 *J. Phys.: Conf. Ser.* **917** 092001

View the [article online](#) for updates and enhancements.

Related content

- [NbN, Nb Double-Layered Base-Electrode Josephson Junctions](#)
Shin Kosaka, Kazuyoshi Kojima, Fujitoshi Shinoki et al.
- [An ab initio study of niobium \(\$n = 2-11\$ \) clusters: structure, stability and magnetism](#)
Ren Feng-Zhu, Wang Yuan-Xu, Zhang Guang-Biao et al.
- [Structure des Nitrures de Niobium](#)
Nobuzo Terao

XPS Depth Profiling of Air-Oxidized Nanofilms of NbN on GaN Buffer-Layers

**A.V. Lubenchenko¹, A.A. Batrakov¹, S. Krause², A.B. Pavolotsky²,
I.V. Shurkaeva¹, D.A. Ivanov¹, O.I. Lubenchenko¹**

¹National Research University "Moscow Power Engineering Institute", Moscow, 111250, Russia

²Chalmers University of Technology, Göteborg, 41296, Sweden

Abstract. XPS depth chemical and phase profiling of an air-oxidized niobium nitride thin film on a buffer-layer GaN is performed. It is found that an intermediate layer of Nb₅N₆ and NbON_x under the layer of niobium oxide is generated.

1. Introduction

The hot electron bolometer mixer (HEB) based on a NbN nanofilm is probably the most sensitive detectors for spectroscopy in the terahertz frequency range above ca. 1 THz [1]. Performance of HEB's depends on uniformity of the 3-6 nm thin NbN layer [2]. The best results have been obtained for monocrystalline NbN films epitaxially grown on GaN buffer-layers. The critical temperature of films on the GaN buffer-layer reached 13.2 K when grown on the hot substrate [3], and 10.4 K when grown over the substrate at the ambient temperature [4].

As a result of oxidation films of niobium and its compounds (initially homogeneous), multilayer and multiphase films are generated. Superconductive functional properties on nano-sized films of niobium compounds worsen by increase of thickness of niobium oxide layers on film surfaces. A sufficient number of works is dedicated to study of niobium oxide films (e. g. [5]). However, there are no papers reporting on phase layer profiling of oxidized nano-sized films of niobium compounds.

At present, depth profiling of thin films is performed using both destructive and non-destructive methods. A review of different profiling methods can be found in [5]. If layers more than tens of nanometers thick are explored, ion sputtering together with some non-destructive method of surface analysis is most frequently used. Ion-surface interaction results not only in sputtering but, due to selective sputtering and ion mixing, in modification of the rest of solid layers up to depths about the projective ion path (few nanometers).

One of the non-destructive profiling methods for nano-sized films is X-ray photoelectron spectroscopy (XPS). The surface area is not only multilayer but layer-multicomponent and multiphase. Layer profiling based on interpretation of XPS spectra of such targets is a complex inverse problem with many parameters that are unknown a priori. To solve this problem correctly, in this work we suggest: 1) a background subtraction method considering difference of energy losses on surface and in volume; 2) using of constant parameters for background calculation and line profiling in all the range of photoelectron spectra; 3) using parameters of line profiles from the Handbook of X-Ray Photoelectron Spectroscopy for pure homogeneous targets; 4) simultaneous interpretation of different lines of the same element using the same model.



2. Experimental Details

In this work, a 5 nm film of NbN on a GaN buffer-layer was studied. Niobium nitride was sputtered onto the substrate by the magnetron method in the experimental setting AJA Orion-5-U-D. The film thickness was controlled by the known sputtering rate confirmed by TEM. After the target was unloaded from the vacuum chamber, it was oxidized in room air at the ambient temperature, and consequently, the film structure changed. This structure change was of interest. Depth profiling of such targets was performed by means of XPS. The XPS spectra were recorded with the help of an electron and ion spectroscopy module based on the platform Nanofab 25 (NT-MDT) by a semi-spherical energy analyzer SPECS Phoibos 225. The energy analyzer was calibrated by samples of Cu, Ag and Au. The energy resolution of the spectrometer at the line Ag 3d5/2 was 0.78 eV for non-monochromatic X-rays of Mg $K\alpha$. All spectra were recorded using a Mg anode, while the energy analyzer worked in the FAT (Fixed Analyzer Transmission) mode. For survey spectra, the deceleration energy setting of the energy analyzer lens was $E_{\text{pass}} = 80$ eV, for detailed spectra it was $E_{\text{pass}} = 20$ eV.

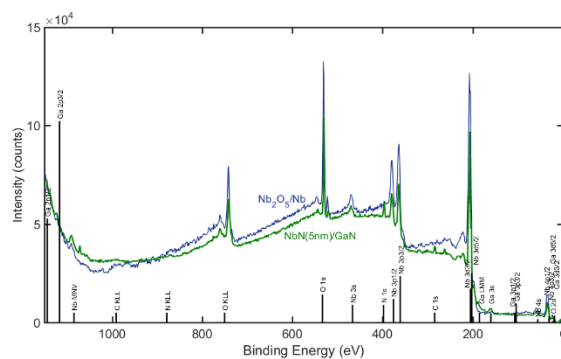


Figure 1. Survey XPS spectrum

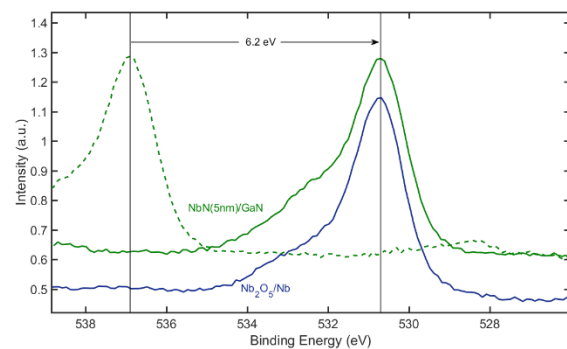


Figure 2. XPS spectrum of line O1s. Dashed line: uncorrected spectrum

Targets with a NbN film on GaN experienced electrical charging during recording of the spectra. The spectra were corrected by the position of the O1s line. For that, spectra of a Nb 100 nm film on a silicon substrate were preliminarily recorded. That film was exposed to natural oxidation; as analysis showed, a layer of Nb₂O₅ 9 nm thick was formed over it. Fig. 1 shows survey XPS spectra, Fig. 2 shows a correction procedure of a NbN (5 nm)/GaN. For a target NbN (5 nm)/GaN, relative concentrations calculated by the standard XPS methods: C – 23%, O – 41%, N – 10%, Nb – 24%, Ga – 2%. However, as far as these data were obtained in assumption of a depth-uniform target, these are only qualitative.

3. Theory

Theoretical explanation of layer profiling methods by means of XPS may be found in papers [7-9]. These methods are based on the standard model of photoelectron scattering in solid [10]. One of the factors of influence on layer profiling calculation accuracy is accuracy of separation of peaks generated by elastically and inelastically scattered electrons. As scattering angles approach sliding angles, surface effects have more and more influence onto the background formed by inelastically scattered electrons. The widely used methods of background subtraction (Shirley [11] and Tougaard [12]) don't consider the difference of inelastic electron scattering in volume and on surface. So the calculation accuracy of layer profiling will be indefinite.

To find the background within an energy range from E_{min} up to E_{max} , considering inelastic scattering on surface as in volume, let us use an approach described in [7]. The Tougaard formula [12] is derived by assumption of depth homogeneity of a target. However, for inelastic scattering a target is always inhomogeneous. Energy losses in surface layers and deep in the target obey different laws. In the first approximation, in a semi-infinite target, let us select a very thin near-surface plane-parallel layer d_s , in which energy losses are determined by excitation of a surface plasmon. In this layer, photoionization

probability is negligible. Out of this layer, energy losses are losses for excitation of a volume plasmon, ionization losses. Using such model and approach [7] we get a formula for background calculation:

$$\text{Background}(E) = A \int_E^{E_{\max}} j(E') x_{\text{SB}}(E - E') dE', \quad (1)$$

where $j(E)$ is an experimentally measured flux of photoelectrons of an energy E , the value A is calculated after finding the background by the energy E_{\min} , $x_{\text{SB}}(\Delta)$ is the differential cross-section of inelastic scattering, orthonormalized per unit of length, named inelastic indicatrix, Δ is the energy loss. The function $x_{\text{SB}}(\Delta)$ depends on inelastic indicatrices of electron scattering in volume $x_{\text{B}}(\Delta)$ and on surface $x_{\text{S}}(\Delta)$ and on $SEP = d_s / \lambda \cos \theta$ (SEP – surface excitation parameter), λ is the inelastic mean free path (IMFP), θ is the angle between the direction to the energy analyzer and the surface normal:

$$x_{\text{SB}}(\Delta) = x_{\text{B}}(\Delta) - \int_0^{\Delta} L_{\text{S}}(\Delta - \varepsilon) x_{\text{B}}(\varepsilon) d\varepsilon + L_{\text{S}}(\Delta), \quad (2)$$

where the function $L_{\text{S}}(\Delta)$ is calculated by the formula

$$L_{\text{S}}(\Delta) \approx \sum_{n=1}^N (-1)^{n+1} \frac{SEP^n}{n!} y_n(\Delta), \quad (3)$$

N is the maximal scattering order considered, $y_n(\Delta)$ are the multiple inelastic indicatrices, $y_1(\Delta) = x_{\text{S}}(\Delta)$, $y_n(\Delta) = \int_0^{\Delta} y_{n-1}(\Delta - \varepsilon) y_1(\varepsilon) d\varepsilon$. If in formula (2) surface energy losses are not considered ($SEP = 0$), the Tougaard formula [14,15] for background is obtained. The calculation formulae for SEP are given in [19,20]. The SEP depends on photoelectron energy, compound and state of the surface.

To calculate the inelastic scattering indicatrix, we suggest to use a formula that is proved to be good in calculation of characteristic electron energy losses [13]:

$$x(\Delta) = \text{norm} \frac{\Delta^{\alpha}}{(\Delta^2 - \varepsilon_{pl}^2)^2 + (\gamma\Delta)^{4-\beta}} \quad (4)$$

where ε_{pl} is the energy of plasma oscillations (plasmon energy); α и β are parameters determining dependence of the function on energy loss; γ is the parameter determining the peak width; the value of norm is found from the normalization condition $\int_0^{\infty} x(\varepsilon) d\varepsilon = 1$.

Fig. 3 shows the results of background subtraction using different methods, for a target of Nb₂O₅/Nb, line Nb 3d. The dash-and-dotted line displays the background according to Shirley, the dotted line is for the Tougaard method using the “universal” inelastic scattering function, the solid line shows the result of the method (1) – (4). The numbers denote the extreme points of various ranges.

The reconstruction method of layer-by-layer profile is based on a target model that results from the history of its production and life. The principle statements of the target model used in this paper:

1) The target consists of few plane layers on a substrate. Each layer is homogeneous and may be multicomponent. Such statement is reasonable because an XPS signal is recorded from a surface area which dimensions are by orders greater than the probing depth. This area depends on focusing of the energy analyzed and geometry of the experiment and it is about 0.1 mm². The probing depth is about 10 nm. So the signal will be measurement area-averaged.

2) Inhomogeneities (islets, interlayer asperities, inclusions, etc.) are layer-averaged. Inhomogeneity rate will define relative concentrations of element phases.

3) After unload from the chamber, the surface is oxidized and oxide and suboxide layers are generated. As far as oxidation progresses from the surface, the oxidation level decreases with depth. Besides that, at the top a hydrocarbon layer will be precipitated.

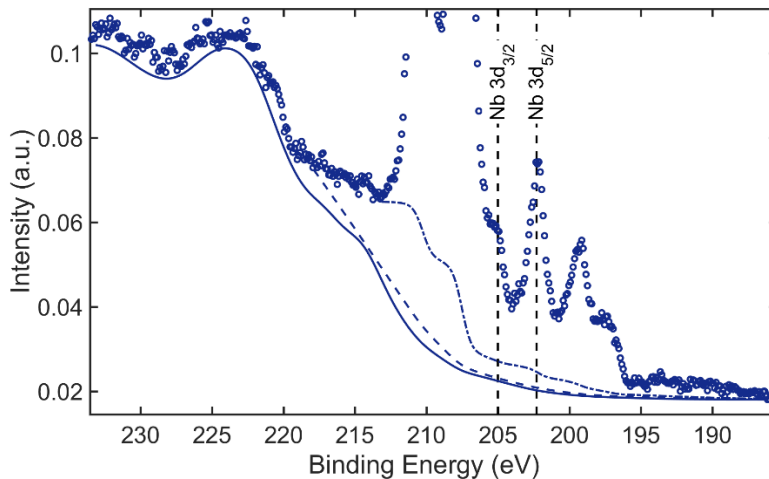


Figure 3. Background calculated by different methods for target of Nb₂O₅/Nb, line Nb 3d. Dash and dots: background calculated using the Shirley method, dots: the Tougaard method, solid line: the method (1) – (4).

The shape of a spectral line of photoelectrons will be determined by a convolution of functions describing the natural line shape and instrumental broadening. The natural line shape will be described the Doniach-Šunjić expression [14] and the instrumental broadening function by the Gauss function. We suggest to take the binding energy and spin-orbital interaction energy for chemically pure elements from the experimental data of the Handbook of X-ray Photoelectron Spectroscopy [15]. The chemical shift energy is almost linearly proportional to the oxidation level, so it is enough to find the chemical shift energy for the most oxidized element. For example, we used a value of 5.31 eV for niobium oxide [16].

Layer thicknesses will be calculated by the formula [17]:

$$d_i = \lambda_i \cos \theta \ln \left(\frac{I_i / (n_i \omega(\gamma) \lambda_i)}{\sum_{j=0}^{i-1} I_j / (n_j \omega(\gamma) \lambda_j)} + 1 \right) \quad (5)$$

where d_i is the thickness of the i -th layer, n is the atomic concentration, $\omega(\gamma)$ is the differential cross-section of photoelectron production [18], γ is the angle between the directions of incident radiation and to the energy analyzer, λ is the IMFP (IMFP is calculated by the TPP2M formula [19]), θ is the angle between the direction to the energy analyzer and the surface normal, I_i is the i -th peak intensity. The layers will be numerated upwards from the substrate. Number 0 means the substrate.

Let us find the depth sensitivity and probing depth of this method. For that a homogeneous layer of niobium oxide Nb₂O₅ on a niobium substrate will be regarded. As far as we determine partial intensities by our method with an accuracy of 1%, let us assume $I_{\text{Nb}_2\text{O}_5} / I_{\text{Nb}} = 1/100$. Then we get from (9) $d_{\text{min}} = 0.1$ nm. Probing depth can be found if assumed $I_{\text{Nb}_2\text{O}_5} / I_{\text{Nb}} = 100/1$. Under formula (9) we calculate $d_{\text{max}} = 13.9$ nm.

To decrease the uncertainty of the number of layers, we suggest to introduce the minimal thickness of a homogeneous layer equal to 0.2 nm. Let us begin calculation from the greatest number of layers possible assuming that every layer is of the same oxidation level. If the calculation shows that a layer is

less than the minimal thickness thick, this layer is added to the nearest one with a greater oxidation level of the main element. The newly constructed layer will be multicomponent. This layer may be regarded as inhomogeneous averaged to a homogeneous layer with an effective thickness. The inhomogeneity degree can be evaluated with the help of relative concentration of the main element of the layer. After that, the layer thicknesses are to be re-calculated. Such approach enables to decrease the number of calculation variants significantly. Then the variants are regarded as profiles calculated with different depth detailing.

4. Results and Discussion

Fig. 4 shows XPS spectra of the line Nb3d, Fig. 5 shows spectra of N1s; the circles show experimental data, the solid line is for theoretical interpretation of the spectrum, the dashed line shows partial theoretical spectra. The line N1s displays different phases of niobium nitride: NbN and NbN_x. Partial intensities on the lines N1s и Nb3d enabled to found a stoichiometric coefficient $x \approx 1.2$ that corresponds to Nb₅N₆.

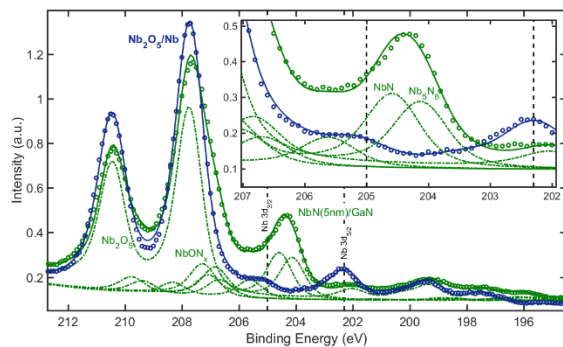


Figure 4. XPS spectra of line Nb3d

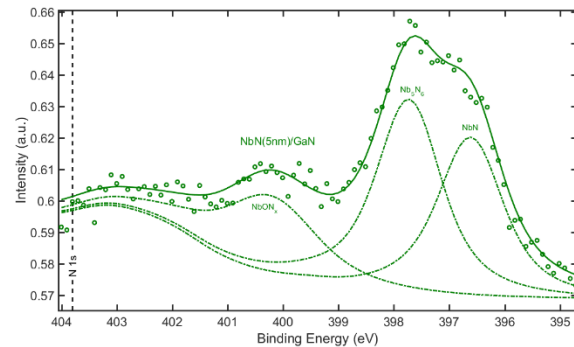


Figure 5. XPS spectra of line N1s

Table 1. Chemical and Phase Depth Profiling of a NbN(5nm)/GaN Target.

	d , nm	Formula
Σ	6.22	
6	0.78	hydrocarbons
5	1.45	Nb ₂ O ₅
4	0.23	0.07 NbO ₂ + 0.93 Nb ₂ O ₃
3	0.78	NbON _x
2	1.30	NbN _x ($x \approx 1.2$)
1	1.68	NbN
Substrate		GaN

Table 1 shows computing results for thicknesses following the formula (5), which accounts for partial intensities obtained by decomposition of the lines N1s, C1s and Nb3d. From the data above, it is found that NbN thickness decreases and various additional phases of niobium nitride appear by oxidizing of the film. Such result is obtained for the first time. Influence of these layers onto HEB's performance needs further research.

5. Conclusions

In this work, a method of chemical and phase layer profiling of multicomponent multilayer films is suggested. The method includes a new subtraction method of background of multiply inelastically scattered electrons considering inhomogeneity of inelastic scattering by depth; a new method of photoelectron line decomposition into constituent peaks considering physical nature of different decomposition parameters; simultaneous solution of the problems of background subtraction and decomposition of a photoelectron line; determination of layer thicknesses of a multilayer target using a

simple formula. On the base of the suggested method, depth chemical and phase profiling of an air-oxidized niobium nitride thin film on a buffer-layer GaN was performed.

References

- [1] Meledin D. et al. 2009 *IEEE Transactions on Microwave Theory and Techniques*. **57.1**. 89.
- [2] Sergeev A., Reizer M. 1996 *Int. J. Mod. Phys.*, **B 10**. 635-667
- [3] Krause S. et al. 2014 *Supercond. Sci. Technol.* **27**. 065009
- [4] Krause S. et al. 2016 *IEEE Transactions on Applied Superconductivity*. **26.3** 1-5
- [5] Darlinski A., Halbritter J. 1987 *Surface and interface analysis*. **10**. 223.
- [6] Galindo R. E. et al. 2010 *Analytical and bioanalytical chemistry*. **396.8**. 2725-2740.
- [7] Cumpson P. J. 1995 *Journal of Electron Spectroscopy and Related Phenomena*. **73.1**. 25-52.
- [8] Palacio C. et al. 2003 *Journal of Electroanalytical Chemistry*. **545**. 53-58.
- [9] Oswald S. et al. 2005 *Applied Surface Science*. **252**. 3–10.
- [10] Macak K. 2011 *Surface and Interface Analysis*. **43.3**. 1581
- [11] Shirley D. A. 1972 *Physical Review*. **B 5.12** 4709
- [12] Tougaard S. 1989 *Surface Science Letters*. **216.3**. A330.
- [13] Afanas'ev V. et al. 2004 *The European Physical Journal B-Condensed Matter and Complex Systems*. **37.1**. 117.
- [14] Doniach S., Sunjic M. 1970 *Journal of Physics C: Solid State Physics*. **3.2**. 285.
- [15] Chastain Jill, King Roger C., Moulder J.F. 1995 *Handbook of X-ray photoelectron spectroscopy: a reference book of standard spectra for identification and interpretation of XPS data*.
- [16] Naumkin A. V, Kraut-Vass A., Powell C.J. 2008 *NIST X-ray photoelectron spectroscopy database*.
- [17] Trifonov A.S. et al. 2015 *Journal of Applied Physics*. **117.12**. 125704.
- [18] Yeh J.J., Lindau I. 1985 *Atomic data and nuclear data tables*. **32.1**. 1.
- [19] Tanuma S., Powell C.J., Penn D.R. 1994 *Surface and Interface Analysis*. **21.3**. 165.